International Conference on Green Energy and Environmental Engineering(GEEE-2017)
International Journal of Control, Energy and Electrical Engineering - CEEE
Vol.4 pp.30-35

Modeling and performance comparison between Boost Converter topologies for Lithium Battery Application in Electric Vehicle

Zaineb KANZARI[1], Jalel KHEDIRI[2], Mohamed JEMLI[3]

[1,3] *Engineering Laboratory of Industrial Systems and Renewable Energies (LISIER), University of Tunis, Higher School of Sciences and Techniques of Tunis, , 5 avenue Taha Hussein, 1008, Tunis, Tunisia*

[1] zkanzari@gmail.com

[3] Jemli-m@voila.fr

[2] *Laboratory of Signal Image and Energy Mastery (SIME), University of Tunis, Higher School of Sciences and Techniques of Tunis, , 5 avenue Taha Hussein, 1008, Tunis, Tunisia*

[2] jalel.khediri@esstt.rnu.tn

***Abstract*— To adapt the voltage levels and to control the energy between the storage elements and the other equipment of an electric vehicle, DC/DC power converters must be interposed. This paper focuses on the modeling and performance comparison between boost converter topologies interfacing a lithium battery and DC link. The design of classic boost converter (BC), interleaved boost converter (IBC) and Interleaved Double Dual Boost converter (IDDBC) is proposed. Simulation results that have been reached put emphasis on the advantages of the IDDBC.**

***Keywords*— Electric vehicle, Lithium battery, Boost Converter, Interleaved Boost Converter, Interleaved Dual Double Boost Converter, Average Model.**

I. INTRODUCTION

Conventional vehicles are in critical condition due to their heavy dependence on petroleum and their contribution to the greenhouse effect. For this reason, the future generation of vehicles must therefore rise this problems.

For this purpose, researchers and vehicle manufacturers focused their work towards electric vehicles.

One of electric vehicle key is batteries [1]. Thanks to their high energy density, they can offer an interesting range. [2],[3] Manufacturers distribute batteries over three large families according to their electrode nature: lead-acid, nickel and lithium batteries. Basic condition must therefore be fulfil by these different technologies in electric vehicles such as:

- A high energy density in order to extend range of electric vehicle
- A stable voltage which leads regular performance.
- Long cycle life which result a lower cost.
- Low maintenance.

Furthermore, Most electric vehicle batteries are lithium due to their performance, especially the energy density [2],[3],[4],[5],[6].

To adapt voltage and current levels and to control the energy between vehicle equipment, a DC/DC converter must be interposed between the storage elements and the DC link[8] [10], [11].

In this work average model and performance of Boost Converter (BC), Interleaved boost Converter (IBC) and Interleaved Double Dual boost converter (IDDBC) are discussed. The aim is to compare the three boost converter topologies.

This paper is organized as follows: Section II describes the Electric vehicle topology. Section III describes the modelling and the sizing of the lithium battery. Section IV presents the average model of the three boost converter topologies. Section V presents simulation results and the comparison between the proposed DC/DC converter, and finally the conclusion is presented in section VI.

II. ELECTRIC VEHICLE TOPOLOGY

The proposed structure used in this paper is the parallel active hybrid topology shown in Fig. 1. The storage elements are connected via a DC/DC power converter to a common DC Bus [8],[9],[10].

This topology adapt the voltage level between the different storage elements and the electric vehicle system through DC/DC converters. A Boost converter is connected to the battery and a Buck-Boost converter is used for the ultracapacitor.

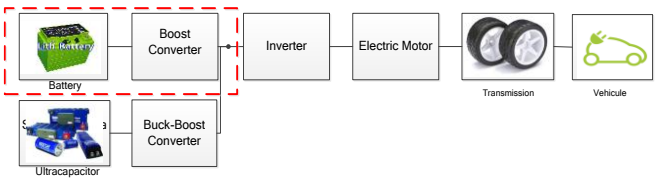

Fig. 1: Diagram of the electric vehicle

In this work, the vehicle is able of producing the required power to accelerate from 0 to100 km/h in 11.5 s and a

maximum speed of 125km/h. The DC bus voltage V_{bus} is 400V.

III. MODELING OF BATTERY DYNAMICS

Several researchers around the world have proposed many kinds of models with varying degrees of complexity and different objectives. Existing battery models can be classified into physical models, analytical models, and equivalent circuit models. [2],[3],[4],[5],[6].

Due to their performance, especially the energy density, most of electric vehicles are powered by lithium-ion (Li-Ion) batteries. [4],[6].

A. PROPOSED MODEL

The dynamic equivalent circuit model is proposed in Fig. 2. The model circuit consists of a DC voltage source, resistances and capacitors. The R_0 represent the resistance of the current collectors on both sides of the electrodes and the two RC networks (R_1, C_1, R_2, C_2) represent the dynamics of the concentration and activation polarization. I_{bat} is the external current of the battery, V_{bat} is the terminal voltage of the battery.[6],[7]

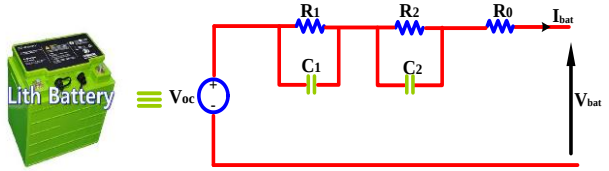

Fig. 2: Equivalent circuit model of a Li-ion battery [7]

In this model, the parameters are dependent on SOC, it can be calculated as Equation (1):

$$SOC = SOC_0 - \int \frac{I_{bat}}{C_{usable}} dt \qquad (1)$$

Where SOC_0 is the initial SOC, and C_{sable} is the usable battery capacity

B. SIZING THE BATTERY MODULE

The battery must be ready to supply the sufficient power so it rolls to a maximum speed of 125 km/h. Thus and according to the characteristics of the vehicle the necessary power produced by the Li-ion battery is 23.48 kw. In this paper, we choose a SAFT Li-ion battery with the following characteristics:

- Nominal voltage (U_{nom}): 3.6 V
- Average capacity C/3 ($C_{nom\text{-}bat}$) : 41Ah
- Minimum capacity C/3($C_{min\text{-}bat}$): 39Ah
- Open circuit voltage(U_{oc}) : 4V
- Weight (We_{bat}): 1.07 Kg
- Volume (V_{bat}): 0.51dm^3

For V_{bat}=120V and V_{bus}=400V, the Li-ion battery parameters are calculated by equations described in Table 1.

TABLE I

LI-ION BATTERY PARAMETERS

Parameters	Equations	VALUE
Series cells	$N_s = \frac{U_{bat}}{U_{bat-oc}}$	30
Courant totale (A)	$I_{tot-bat} = \frac{P_{ch-bat}}{U_{bat}}$	195.7
Parallel branches	$N_p = \frac{I_{tot-bat}}{I_{bat-\min}}$	2
Battery cells number	$N_{tot-bat} = N_p \times N_s$	60
Battery module weight (Kg)	$We_{bat-tot} = We_{bat} \times N_{tot-bat}$	64.2
Battery module volume (dm^3)	$V_{bat-tot} = V_{bat} \times N_{tot-bat}$	30.6
Total energy (wh)	$E_{bat-tot} = N_p \times C_{nom-bat} \times N_s \times U_{nom-bat}$	8856

IV. DIFFERENT TOPOLOGIES OF BOOST CONVERTER

The chosen converter is a boost converter which allows the increase of the lithium battery output voltage in order to supply the DC bus.

A. CLASSIC BOOST CONVERTER

Fig. 3 shows the electrical circuit of a classic boost converter.

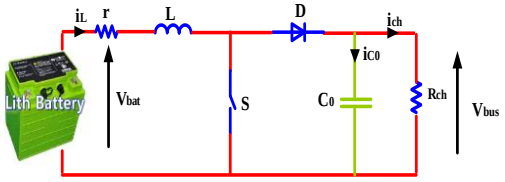

Fig. 3: Circuit design of a classic Boost Converter

There is two modes of operation:

- During the first interval : S is ON and D is OFF :

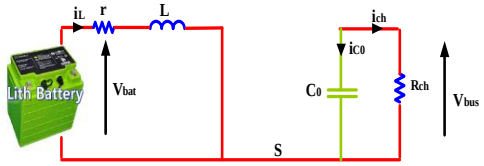

Fig. 4: Configuration of the Boost Converter for S:ON

The state space model and matrices are:

$$\dot{x} = A_1 x + B_1 u \qquad (2)$$

$$y = C_1 x \qquad (3)$$

With :

$x = [i_L \; V_{bus}]^T$; $u = V_{bat}$; $y = V_{bus}$

In that case:

$$A_1 = \begin{pmatrix} -\frac{r}{L} & 0 \\ 0 & -\frac{1}{R_{ch}C_0} \end{pmatrix}; \quad B_1 = \begin{pmatrix} \frac{1}{L} \\ 0 \end{pmatrix}; \quad C_1 = \begin{pmatrix} 0 \\ 1 \end{pmatrix}^T \tag{4}$$

- During the second interval S is OFF and D is ON :

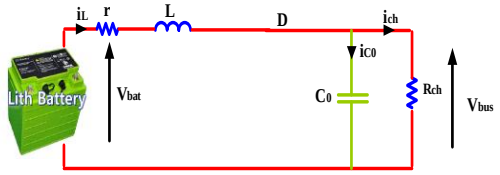

Fig. 5: Configuration of the Boost Converter for D:ON

The state space model and matrices are:

$$\dot{x} = A_2 x + B_2 u \tag{5}$$

$$y = C_2 x \tag{6}$$

In this case:

$$A_2 = \begin{pmatrix} -\frac{r}{L} & -\frac{1}{L} \\ \frac{1}{C_0} & -\frac{1}{R_{ch}C_0} \end{pmatrix}; \quad B_2 = \begin{pmatrix} \frac{1}{L} \\ 0 \end{pmatrix}; \quad C_2 = \begin{pmatrix} 0 \\ 1 \end{pmatrix}^T$$

Then the averaged model is:

$$\dot{x} = Ax + Bu \tag{7}$$

$$y = Cx \tag{8}$$

With:

$$A = d.A_1 + (1-d)A_2 \tag{9}$$

$$B = d.B_1 + (1-d)B_2 \tag{10}$$

$$C = d.C_1 + (1-d)C_2 \tag{11}$$

d: duty cycle

We obtain:

$$A = \begin{pmatrix} -\frac{r}{L} & -\frac{(1-d)}{L} \\ \frac{1-d}{C_0} & -\frac{1}{R_{ch}C_0} \end{pmatrix}; \quad B = \begin{pmatrix} \frac{1}{L} \\ 0 \end{pmatrix}; \quad C = \begin{pmatrix} 0 \\ 1 \end{pmatrix}^T$$

B. INTERLEAVED BOOST CONVERTER:

The circuit diagram of an IBC is shown in Fig. 6. The configuration is composed of switches S_1 and S_2, inductors L_1 and L_2, diodes D_1 and D_2, Capacitor C_0 and load resistor R_{ch}.

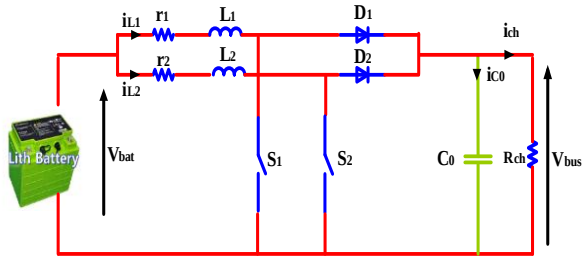

Fig. 6: Interleaved Boost Converter

The power switches S_1 and S_2 have 180° phase difference [11], [12].

There are two duties cycle of operation converter: for d<0.5 and d>0.5.

For d>0.5 the converter has four modes of operation and the switching states are given in Table 2.

TABLE II

STATES OF SWITCHES

Stages	Mode of Operation	S_1	S_2	D_1	D_2
1	$0 < t < Ts(d - \frac{1}{2})$	1	1	0	0
2	$Ts(d - \frac{1}{2}) < t < \frac{Ts}{2}$	1	0	0	1
3	$\frac{Ts}{2} < t < dTs$	1	1	0	0
4	$dTs < t < Ts$	0	1	1	0

Fig. 7 shows the inductor current waveforms of the IBC for d>0.5 :

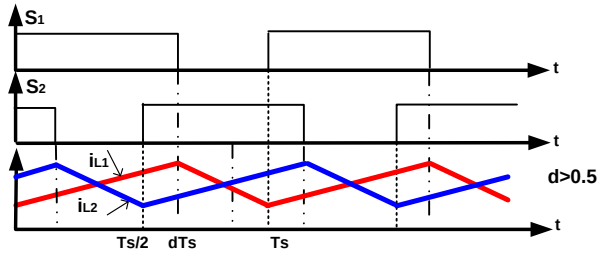

Fig. 7: Inductor Current of IBC Converter for d > 0.5

The states are shown in Fig. 8:

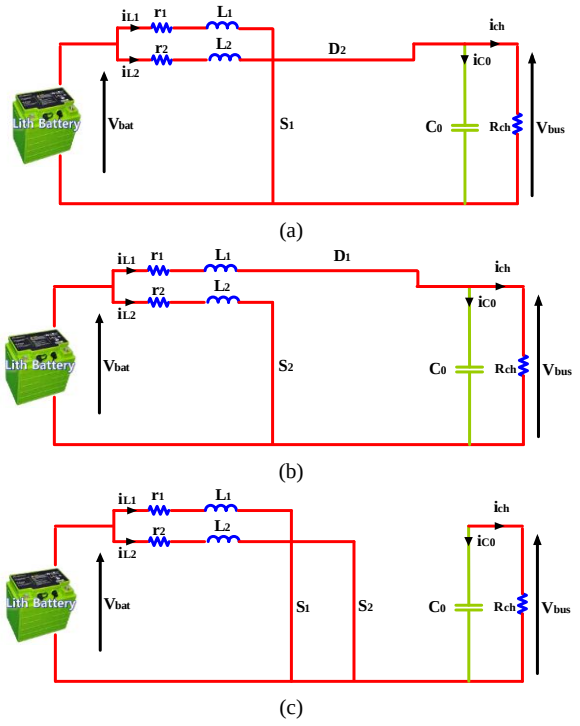

Fig. 8: (a) S1,D2: ON (b) S2,D1:ON (c) S1,S2:ON

State-space average models are :

$$\dot{x} = A_{2i}x + B_{2i}u \tag{12}$$

$$y = C_{2i}x \tag{13}$$

Where i is the stage rank, Then:

$$x = [i_{L1}\ i_{L2}\ V_{bus}]^T ; u = V_{bat} ; y = V_{bus}$$

Matrices are given by:

$$A_{21} = A_{23} = \begin{pmatrix} -\frac{r_1}{L_1} & 0 & 0 \\ 0 & -\frac{r_2}{L_2} & 0 \\ 0 & 0 & -\frac{1}{R_{ch}C_0} \end{pmatrix} \quad A_{22} = \begin{pmatrix} -\frac{r_1}{L_1} & 0 & 0 \\ 0 & -\frac{r_2}{L_2} & -\frac{1}{L_2} \\ 0 & \frac{1}{C_0} & -\frac{1}{R_{ch}C_0} \end{pmatrix}$$

$$A_{24} = \begin{pmatrix} -\frac{r_1}{L_1} & 0 & -\frac{1}{L_1} \\ 0 & -\frac{r_2}{L_2} & 0 \\ \frac{1}{C_0} & 0 & -\frac{1}{R_{ch}C_0} \end{pmatrix}$$

$$B_{21} = B_{22} = B_{23} = B_{24} = \begin{bmatrix} \frac{1}{L_1} & \frac{1}{L_2} & 0 \end{bmatrix}^T$$

$$C_{21} = C_{22} = C_{23} = C_{24} = (0 \quad 0 \quad 1)$$

Taking the average of the above state models results in the following average state-space model :

$$\dot{x} = A_2x + B_2u \tag{14}$$

$$y = C_2x \tag{15}$$

$$A_2 = A_{21}(d - \frac{1}{2}) + A_{22}(1-d) + A_{23}(d - \frac{1}{2}) + A_{24}(1-d) \tag{16}$$

$$B_2 = B_{21}(d - \frac{1}{2}) + B_{22}(1-d) + B_{23}(d - \frac{1}{2}) + B_{24}(1-d) \tag{17}$$

$$C_2 = C_{21}(d - \frac{1}{2}) + C_{22}(1-d) + C_{23}(d - \frac{1}{2}) + C_{24}(1-d) \tag{18}$$

The corresponding A_2, B_2 and C_2 matrices are :

$$A_2 = \begin{pmatrix} -\frac{r_1}{L_1} & 0 & -\frac{(1-d)}{L_1} \\ 0 & -\frac{r_2}{L_2} & -\frac{(1-d)}{L_2} \\ \frac{(1-d)}{C_0} & \frac{(1-d)}{C_0} & -\frac{1}{R_{ch}C_0} \end{pmatrix} ; B_2 = \begin{bmatrix} \frac{1}{L_1} & \frac{1}{L_2} & 0 \end{bmatrix}^T$$

$$C_2 = [0 \quad 0 \quad 1]$$

C. The Interleaved Double Dual Boost converter

The circuit diagram of an IDDBC is shown in Fig. 9. The topology consists of two single boost converters with input coupled inversely [13]. As the IBC, the control switching is adjusted by Ts/2where Ts is the switching period.

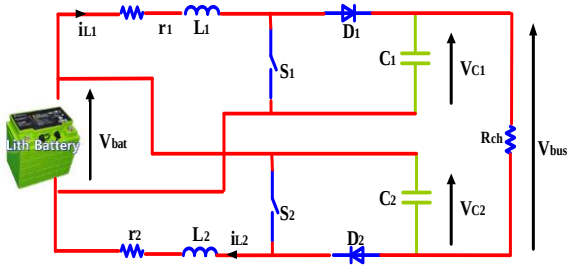

Fig. 9: Interleaved Double Dual Boost converter

The output voltage Vbus is given by :

$$V_{bus} = V_{C1} + V_{C2} - V_{bat} \tag{19}$$

The input current delivred by the battery is given by :

$$i_{bat} = i_{L1} + i_{L2} - i_{bus} \tag{20}$$

Based on table 2, the states are shown in Fig. 10:

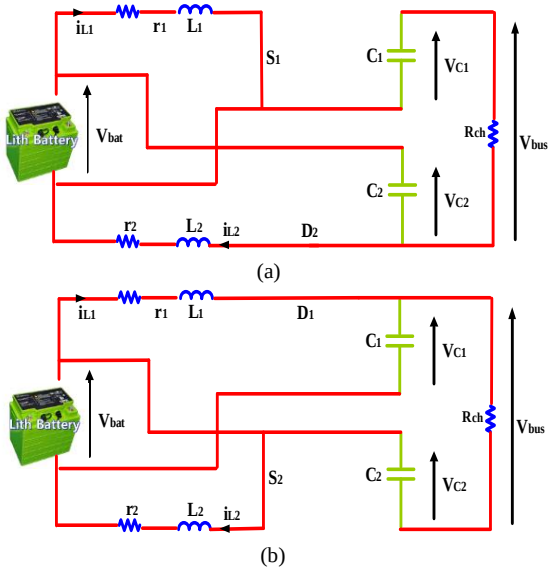

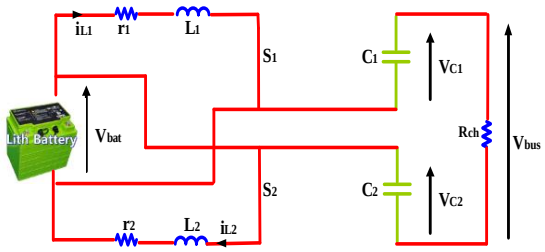

(c)

Fig. 10: (a) S1,D2: ON (b) S2,D1:ON (c): S1,S2:ON

For: $x=[i_{L1}\ V_{C1}\ i_{L2}\ V_{C2}]^T; u=V_{bat}; y=V_{bus}$

Based on equation (12),(13) matrices are given by:

$$A_{21}=A_{23}=\begin{pmatrix} -\frac{r_1}{L_1} & 0 & 0 & 0 \\ 0 & -\frac{1}{R_{ch}C_1} & 0 & -\frac{1}{R_{ch}C_2} \\ 0 & 0 & -\frac{r_2}{L_2} & 0 \\ 0 & -\frac{1}{R_{ch}C_2} & 0 & -\frac{1}{R_{ch}C_2} \end{pmatrix} A_{22}=\begin{pmatrix} -\frac{r_1}{L_1} & 0 & 0 & 0 \\ 0 & -\frac{1}{R_{ch}C_1} & 0 & -\frac{1}{R_{ch}C_2} \\ 0 & 0 & -\frac{r_2}{L_2} & -\frac{1}{L_2} \\ \frac{1}{C_2} & 0 & \frac{1}{C_2} & -\frac{1}{R_{ch}C_2} \end{pmatrix}$$

$$A_{24}=\begin{pmatrix} -\frac{r_1}{L_1} & -\frac{1}{L_1} & 0 & 0 \\ \frac{1}{C_1} & -\frac{1}{R_{ch}C_1} & 0 & -\frac{1}{R_{ch}C_1} \\ 0 & 0 & -\frac{r_2}{L_2} & 0 \\ 0 & -\frac{1}{R_{ch}C_2} & 0 & -\frac{1}{R_{ch}C_2} \end{pmatrix}$$

$$B_{21}=B_{22}=B_{23}=B_{24}=\begin{bmatrix} \frac{1}{L_1} & \frac{1}{R_{ch}C_1} & \frac{1}{L_2} & \frac{1}{R_{ch}C_2} \end{bmatrix}^T;$$

$$C_{21}=C_{22}=C_{23}=C_{24}=[0\quad 1\quad 0\quad 1]$$

$$D_{21}=D_{22}=D_{23}=D_{24}=[-1]$$

Based on equation (14),(15), in this case:

$$A_2=A_{21}(d-\frac{1}{2})+A_{22}(1-d)+A_{23}(d-\frac{1}{2})+A_{24}(1-d) \quad (21)$$

$$B_2=B_{21}(d-\frac{1}{2})+B_{22}(1-d)+B_{23}(d-\frac{1}{2})+B_{24}(1-d) \quad (22)$$

$$C_2=C_{21}(d-\frac{1}{2})+C_{22}(1-d)+C_{23}(d-\frac{1}{2})+C_{24}(1-d) \quad (23)$$

$$D_2=D_{21}(d-\frac{1}{2})+D_{22}(1-d)+D_{23}(d-\frac{1}{2})+D_{24}(1-d) \quad (24)$$

The corresponding A_2, B_2 C_2 and D_2 matrices are :

$$A_2=\begin{pmatrix} -\frac{r_1}{L_1} & -\frac{(1-d)}{L_1} & 0 & 0 \\ \frac{(1-d)}{C_1} & -\frac{1}{R_{ch}C_1} & 0 & -\frac{1}{R_{ch}C_1} \\ 0 & 0 & -\frac{r_2}{L_2} & -\frac{(1-d)}{L_2} \\ 0 & -\frac{1}{R_{ch}C_2} & \frac{(1-d)}{C_1} & -\frac{1}{R_{ch}C_2} \end{pmatrix}$$

$$B_2=\begin{bmatrix} \frac{1}{L_1} & \frac{1}{R_{ch}C_1} & \frac{1}{L_2} & \frac{1}{R_{ch}C_2} \end{bmatrix}^T; C_2=[0\quad 1\quad 0\quad 1]; D_2=[-1]$$

V. MATLAB/SIMULINK SIMULATION

In this paper, we modeled in matlab the average model of the different topologies of the boost converter. Closed loop control is used with classic PI regulators. The PI controller is configured to regulate the output voltage (V_{bus})

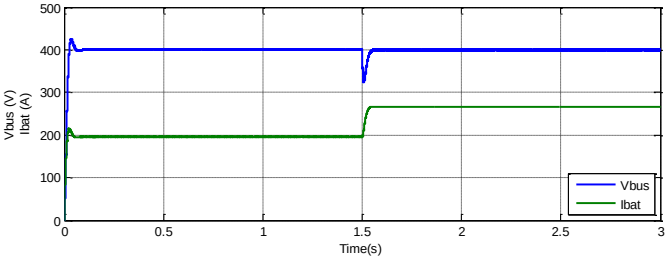

Fig. 11: waveform of output voltage and battery current in changed load

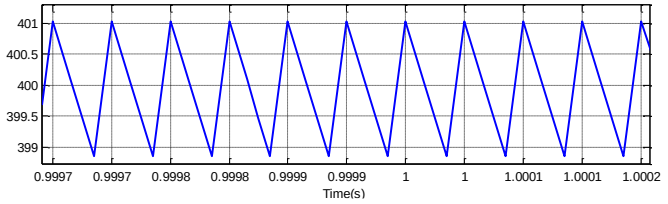

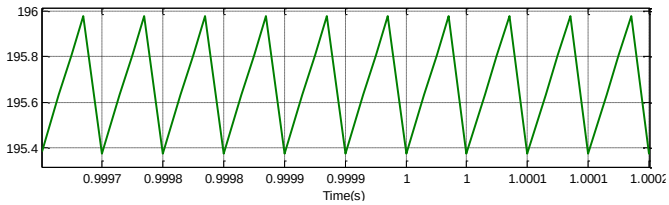

Fig. 12: Inductor current ripple and output voltage ripple of the BC

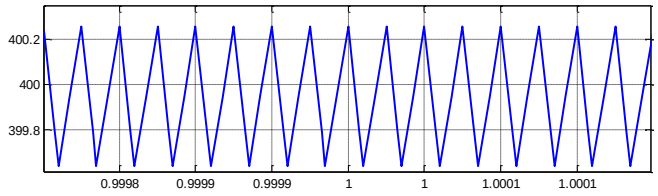

Fig. 13: Output voltage ripple of the IBC

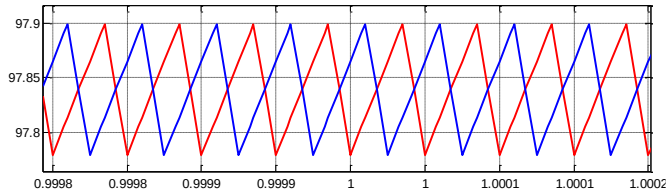

Fig. 14: Inductors currents (i_{L1}, i_{L2}) of IBC

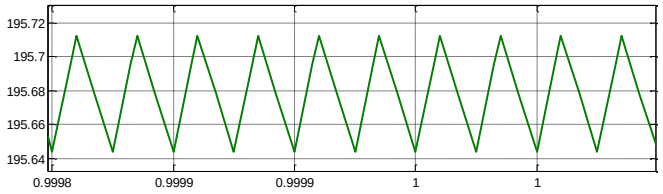

Fig. 15: Inductor current ripple of IBC

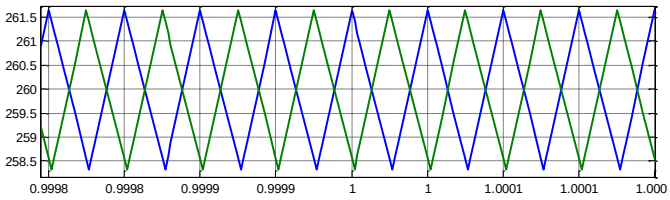

Fig. 16: Outputs Voltages (V_{C1}, V_{C2}) ripple of IDDBC

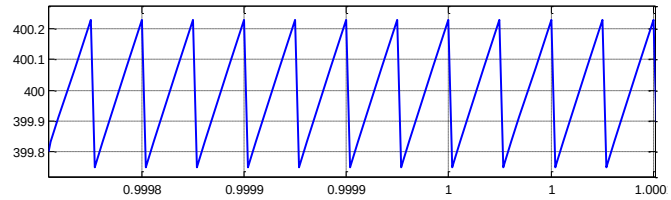

Fig. 17: Output voltage (V_{bus}) ripple of the IDDBC

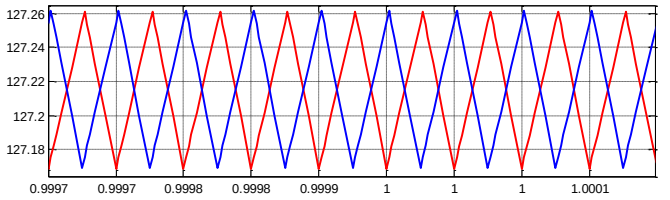

Fig. 18: Inductors currents (i_{L1}, i_{L2}) of IDDBC

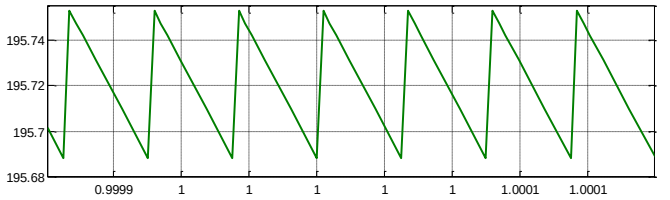

Fig. 19: Inductor current ripple of IDDBC

TABLE III

COMPARISON BETWEEN BC, IBC AND IDDBC

PARAMETERS	**BC**	**IBC**	**IDDBC**
Duty Cycle	0.7	0.7	0.5385
Inductor(μH)	510	255	255
Capacitor (μF)	611	611	305
Input Current Ripple(A)	0.6	0.065	0.06
Output Voltage Ripple(V)	2.1	0.59	0.49
Efficiency (%)	97,31	98,9	99,98

It is clear from the table III that the ripples of output current and output voltage are reduced for IDDBC compared with BC and IBC. These results shows the advantages of IDDBC having the highest efficiency and the lower duty cycle.

VI. CONCLUSION

This paper discusses the principle, operating modes and mathematical model of various boost converter topologies. The waveforms of BC, IBC and IDDBC have been simulated. Using these results, the IDDBC has advantages based on comparison with BC and IBC such as the decrease of the size of the filtering component and the reduction of the input current and output voltage ripple. Due to the decrease of the current ripple at the input the stress on the battery will be reduced. The decrease of the duty cycle can improve the efficiency of the IDDBC. Therefore, from the comparative study, the IDDBC proves to be a promising topology for Electric Vehicle Application.

REFERENCES

[1] R. Xiong, H. He, F. Sun, and K. Zhao, "Evaluation on state of charge estimation of batteries with adaptive extended Kalman filter by experiment approach," IEEE Trans. Veh. Technol., vol. 62, pp. 108-117, Jan. 2013.

[2] L. Lin, N. Kawarabayashi, M. Fukui, S. Tsukiyama, and I. Shirakawa, "A practical and accurate SOC estimation system for lithium ion batteries," in Proc. 17th International Meeting on Lithium Batteries,, June. 2014.

[3] Arnab Kundu, Rajiv Kumar Utsav, José Debangshu Das, and Arnab Adhikari, "A Comparative Analysis of Optimased Lithium-1on its Application", International Journal of Emerging Technology and Advanced Engineering, Volume 4, Issue 4, April 2014.

[4] S. Wijewardana1, "New Dynamic Battery Model for Hybrid Vehicles", International Journal of Emerging Technology and Advanced Engineering, Volume 4, Issue 4, April 2014.

[5] O. Tremblay, L. Dessaint, Experimental Validation of a Battery Dynamic Model for EV Applications, World Electric Vehicle Journal 2009, Stavanger, Norway.

[6] F. Baronti, G. Fantechi, L. Fanucci, E. Leonardi, R. Roncella, R. Saletti, and S. Saponara, "State-of-charge estimation enhancing of lithium batteries through a temperature-dependent cell model," in Proc. Applied Electronics (AE), pp.1-5, 2011.

[7] M. Chen, and G. A. Rincon-Mora, "Accurate electrical battery model capable of predicting runtime and I-V performance," IEEE Trans. On Energy Conversion, vol.21, no.2, pp.504-511, 2011.

[8] H.S.Khaldi and A.C.Ammari "Design and Comparison of two DC/DC Converter Topologies Interfacing a Hybrid Energy Storage System to the DC Bus „" International Conference on Control, Engineering & Information Technology (CEIT"14) , Tunisia 2014.

[9] M. Amari, F. Bacha and J. Ghouili "Average Model for an Interleaved DC/DC Boost for Fuel Cell Electrical Vehicle", International Journal of Emerging Technology and Advanced Engineering, Vol. 5, Issue 1, January 2016.

[10] H.S.Khaldi and A.C.Ammari "Design of an Hybrid Battery/Super-capacitors Energy Storage System for Hybrid Electric Vehicles", Life Science Journal, 2014.

[11] M. Wegmuller, J. P. von der Weid, P. Oberson, and N. Gisin, "Design And Simulation Of Two Phase Interleaved Boost Converter For Photovoltaic Generation System," International Journal of Applied Engineering Research, Vol. 10 No.4, 2015.

[12] N. Benyahia, H. Denoun, A. Badji, M. Zaouia, T. Rekioua, N. Benamrouche and D. Rekioua, "MPPT controller for an interleaved boost dc dc converter used in fuel cell electric vehicles" international journal of hydrogen energy, 2014

[13] Fellipe S. Garcia, José A. Pomilio, and Giorgio Spiazzi, "Modeling and Control Design of the Interleaved Double Dual Boost Converter," IEEE Transactions On Industrial Electronics, VOL. 60, NO. 8, AUGUST 2013.

ISSN 2356-5608